

Spectral Doppler Processing and Quantification in the Context of Progressive Aortic Stenosis

By:

Lily R. Thomson
Sophie E. Phillips

Advisors:

Jonathan Lindner, Department of Cardiovascular Medicine
John A. Hossack, Department of Biomedical Engineering

Word count: 3729

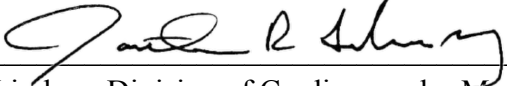
Number of figures: 6

Number of tables: 1

Number of equations: 0

Number of Supplements: 4

Number of References: 18

Approved 
Dr. Jonathan Lindner, Division of Cardiovascular Medicine

Date May 6, 2025

Approved 
Dr. John A. Hossack, Department of Biomedical Engineering

Date May 7th 2025

Spectral Doppler Processing and Quantification in the Context of Progressive Aortic Stenosis

Sophie E. Phillips^{a,1*}, Lily R. Thomson^{a,2*}, John A. Hossack^{b,3}, Bethany Gholson^{c,4}, Jeesoo Lee^{d,5}, Jonathan R. Lindner^{c,6}

^a Fourth Year Biomedical Engineering Undergraduate, University of Virginia

^b Department of Biomedical Engineering, University of Virginia

^c Division of Cardiovascular Medicine, University of Virginia

^d Feinberg School of Medicine, Northwestern University

¹ Correspondence: nsj9fx@virginia.edu

² Correspondence: fze2ex@virginia.edu

³ Correspondence: jh7fj@virginia.edu4

⁴ Correspondence: BAP5B@uvahealth.org

⁵ Correspondence: eesoolee@northwestern.edu

⁶ Correspondence: JRL5Y@uvahealth.org

*Authors contributed equally

Abstract

In mild or moderate aortic stenosis (AS), regional microdomains of high-velocity flow may accelerate progression of AS through shear signaling. These domains can appear as low-amplitude high-velocity (LAHV) signals on continuous wave (CW) Doppler across the aortic valve, often described as “fuzz.” Our aim was to develop a method for quantifying LAHV signals through image processing of velocity-intensity maps. We enrolled 30 patients with mild to moderate AS and performed comprehensive echocardiography. The developed MATLAB program processes the Doppler images by denoising, plotting a velocity-amplitude histogram, and calculating the area under the curve (AUC) for LAHV signals beyond the peak velocity of the main CW jet. These values were compared to expert visual grading of LAHV signals and blood markers of shear activation, including Von Willebrand factor ultralarger multimers (UL-VWF). The program reliably identified an AUC distinct from the signal’s main body. Patients visually identified as having LAHV domains had significantly higher AUC values than those without (3393±1079 vs 1864±693, $p < 0.001$). Subjective LAHV grade correlated well with AUC ($p = 0.0002$) and AUC normalized to gain (average intensity of profile) ($p = 0.001$). Several shear-activation markers correlated linearly with LAHV including activation specific staining of GPIIb/IIIa and plasma UL-VWF. Novel off-line image analysis allows quantification of LAHV signals from CW Doppler of the aortic valve without requiring raw Doppler data. This approach identifies patients with markers of increased valve shear. Future studies will evaluate the ability of this program to identify patients at high risk for progression.

Keywords: Aortic stenosis, shear stress, continuous wave Doppler, high-velocity flow, image processing, Von Willebrand factor, platelet activation, velocity-intensity mapping

Introduction

Aortic stenosis (AS) is a type of heart valve disease that is present in about 5% of the population at age 65, with these numbers increasing with age.¹ This disease

occurs when the aortic valve narrows and thickens, reducing the area for blood to move through from the left ventricle to the aorta.² With each systole, the cusps/leaflets of the valve don’t open completely, decreasing the area

available for blood flow. Thus, the heart needs to work harder to pump blood, which can lead to left ventricle thickening and enlargement. This will weaken the heart muscle and can lead to heart failure and death if left untreated.

The aortic structure is largely maintained by valvular interstitial cells (VICs) that produce the protein scaffolds needed for valve flexibility and strength in the face of high pressure. Aortic stenosis is caused by a process that involves osteogenic and myofibroblastic transformation of VICs that then produce abnormal amounts or types of matrix and calcium in the leaflets, following shear or mechanical stress to the valve.³ Risk factors for AS include high cholesterol and triglyceride levels, high blood pressure, smoking, Type 1 diabetes, obesity, and a high saturated fat diet (Figure 1).

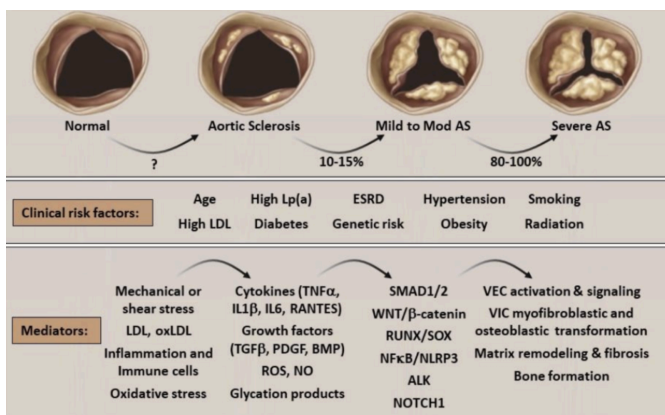


Figure 1. Schematic of progressive aortic valve calcification along with clinical risk factors and biological mediators at each step.⁴

Less commonly, aortic stenosis can be caused by a congenital heart defect, where children are born with either one, two, or four cusps in the aortic valve. Additionally, rheumatic fever can leave scar tissue on the aortic valve, which is a rough surface where calcium deposits can collect.⁵ A range of cardiovascular imaging techniques can be used to diagnose aortic stenosis, including a transthoracic echocardiogram (TTE), electrocardiograph (ECG), magnetic resonance imaging (MRI), and more.⁶ While a patient can live with AS and not experience symptoms, mortality rates are over 90% within the first few years after the onset of symptoms if left untreated.⁷

Current Procedures for Treating Aortic Stenosis

The current treatment options for AS include a balloon valvuloplasty, transcatheter aortic valve replacement (TAVR), or an aortic valve replacement. In a balloon valvuloplasty, a balloon attached to a catheter is

inserted into the narrowed valve and inflated with a sterile liquid mixture to increase blood flow.⁸ Though this procedure is minimally invasive and low risk, the symptom relief only lasts for several months to a year. A TAVR, typically only done in patients with severe AS, is also minimally invasive, using a catheter to deliver a new heart valve instead of needing to perform open heart surgery.⁹ The TAVR is comparable to a surgical AVR. However, there are risks associated with both TAVR and surgical AVR including bleeding, infection, stroke, or even death.^{10,11} Additionally, these treatments all cost thousands to hundreds of thousands of dollars, creating significant financial barriers for uninsured patients and posing challenges for healthcare systems in ensuring equitable access to life-saving interventions.¹² Aside from these treatments, there is medical management, in which medications can be used to alleviate symptoms, but none exist that stop the progression of the disease. Thus, there remains a significant demand for a nonsurgical therapy to delay or even prevent the need for a valve replacement. A treatment of this kind would revolutionize care, offering relief and extending survival for patients who cannot undergo surgery or for whom surgical risks outweigh the benefits.

Innovation

Current and potential areas of investigation for nonsurgical innovations include pharmacological interventions, gene/molecular therapies, catheter-based preventative therapies, and finding biomarkers for early intervention.¹³ Identifying markers of rapid AS progression could help tailor earlier, nonsurgical interventions. In order to develop drug therapies for AS, there is a need to understand mechanisms behind rapid progression of disease versus slow progression of disease. This project, and the larger one encompassing it, aims to further understand the mechanisms driving valve calcification and inflammation. While the clinical factors that lead to AS and the cellular events that lead to valve calcification and fibrosis are largely understood, a successful pharmacological treatment to slow disease progression does not yet exist.⁴ Statins, cholesterol-lowering drugs, have been the most extensively studied pharmacological treatment for AS. However, since many clinical trials have concluded that they offer no significant clinical benefit in slowing AS progression, the American Heart Association/American College of Cardiology and the European Society of Cardiology guidelines do not recommend using these drugs to treat progressive AS.¹⁴

Preliminary work.

The larger AS study encompassing this capstone project is focused on the role of Von Willebrand Factor (VWF) and platelet adhesion in disease progression, which could serve as a target for a successful pharmacological treatment.⁴ The first aim of this larger study is to use imaging to study VWF-mediated platelet adhesion in AS progression in mouse models.¹⁵ Contrast-enhanced ultrasound (CEU) is used to track targeted microbubbles for real-time imaging of platelet adhesion and quantify the extent of VWF-mediated platelet adhesion under pathological shear conditions. The preliminary studies have established that LDLR^{-/-}AD13^{-/-} mice, which lack the ability to cleave endothelial VWF, develop more pronounced AS. This is evidenced by increased platelet adhesion and enhanced VWF A1 domain exposure, promoting fibrotic and osteogenic signaling pathways that contribute to valve thickening and calcification. Future work will focus on extending the study time-frame and introducing therapeutic interventions to test the causal role of platelet adhesion.

The second aim of this study is to test whether treatments that reduce VWF can slow AS progression, such as antioxidants and drugs that inhibit VWF multimerization.⁴ Results from LDLR^{-/-}AD13^{-/-} mice treated with apocynin, a Nox2 inhibitor, indicate reduced valve thickening, osteogenic transformation, and platelet adhesion. Building on these findings, the aim will test apocynin and NAC for their potential to suppress excess endothelial-associated VWF and slow AS progression.

The third aim of this study is to conduct a clinical trial to evaluate if markers of abnormal VWF proteolysis and platelet-derived factors can predict AS progression in patients. Pilot analyses have demonstrated that abnormal VWF cleavage correlates with progressive valve changes. Novel Doppler-derived high-risk shear markers and 4D MRI of 3D-printed valve replicas will be used to validate these findings in vivo.⁴ The planned 4-5 year study involves 40 adult patients with mild to moderate AS, evaluating echocardiographic determinants of high-risk patterns of trans-catheter shear that influence VWF activation.

Common to all of these aims is the importance of high valvular shear which can lead to these determinantal biologic processes. This Capstone project contributes to the assessment of CW spectral Doppler signals beyond the typical analysis and further investigates these mechanisms.

Project Aims.

Continuous wave (CW) spectral Doppler imaging can be used to determine blood flow velocities through the

aortic valve, especially when evaluating high-velocity pathological lesions.¹⁶ These signals can be quantified to determine blood volumes, pressure gradients, valve areas, and intracardiac pressures —key metrics for diagnosing and studying aortic stenosis. Sonographers can extract mean and peak velocities from spectral Doppler images and modify parameters like time-velocity intervals. However, there are no standard clinical tools to produce a velocity-amplitude spectrum from these images, as diagnostic emphasis prioritizes velocity-based metrics rather than amplitude analysis. Thus, the amplitude of the Doppler signal (reflecting blood cell density and turbulence) is generally displayed qualitatively, not quantitatively. Producing such velocity-amplitude spectrums could offer insights into blood flow turbulence and information about shear forces relevant to diseases like AS.

Spectral Doppler images show time on the x-axis and velocity on the y-axis (of blood flow towards or away from the transducer).¹⁶ When assessing CW spectral Doppler signals, often there is a very dense main velocity profile, but also a small amount of very high velocity low-intensity signal at the “tip” of the profile

which is conventionally ignored.¹⁵ However, these areas of high velocity could correspond to small microdomains of high resistance and high shear through the valve. The presence of high shear stress can damage the valve and lead to excess VWF on the leaflets. VWF is a large glycoprotein involved in hemostasis or the body’s way of stopping bleeding from an injury.¹⁷ A vascular injury can expose VWF bound to subendothelial collagen and trigger events that lead to platelet adhesion and recruitment to repair the damaged endothelium. Given that this protein contributes to platelet adhesion and clotting, we believe that it can further contribute to AS. Thus, this high shear could be a marker of abnormal VWF proteolysis and/or indicative of a patient’s likelihood of developing rapidly progressing AS.⁴ To investigate this, the research team needs a program that can analyze the spectral Doppler images and quantify the LAHV signal at the “tip” of the main velocity profile and

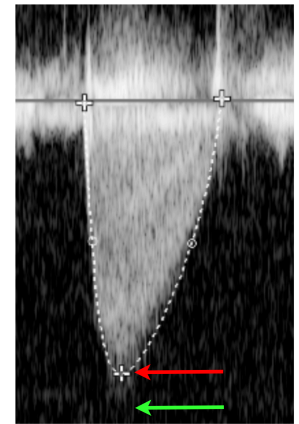


Figure 2. Doppler waveform with red arrow at main jet peak velocity; green arrow marks LAHV signal.

quantify these signals compared to the main velocity profile (Figure 2).¹⁰

This project uses advanced signaling techniques to address the current limitations in detecting and quantifying regions on Doppler images. It also contributes to the broader study on AS, focusing on the role of VWF and platelet adhesion in disease progression. Ultimately, these findings could support the preliminary work discussed above.

Methods

A custom MATLAB script was developed to analyze Doppler echocardiography images and quantify intensity-velocity profiles associated with blood flow patterns (Supplementary Figure 1). Prior to execution, the MATLAB script (Script.m) was placed in the same directory as a folder containing Doppler ultrasound images (in .png or .jpeg format), which served as the input data. The Doppler images were acquired using *Philips Ultrasound* technology from patients enrolled in this clinical trial.

Image Preprocessing

Upon launching the program, the user is prompted to specify the name of the Doppler image to be analyzed. The script first displays the selected image and allows the user to manually define a rectangular region in the background, from which average pixel intensity was subtracted to normalize the image and correct for background signal noise.

Velocity Scale Calibration

Since each image has a velocity bar scale to the right of the Doppler signal, the velocity values must be scaled appropriately to the pixel values on the y-axis (each image is a matrix of (m,n) pixel values). The MATLAB `ginput(n)` allows the user to click “n” locations on the image, and a pixel coordinate will be returned. The user is asked to interactively select two key points on the image's velocity scale: the “0 cm/s” reference and a maximum velocity value of “300 cm/s.” These reference points are used to map pixel positions on the vertical axis to physical velocity values, enabling pixel-to-velocity calibration to determine what a 1 cm/s step in velocity corresponds to in pixel size.

Region of Interest Isolation

Subsequently, the user defines the spatial boundaries of the velocity profile by selecting the left and right edges, as well as the baseline and bottom edge of the region of interest (ROI). The image is masked accordingly

to isolate only the profile of interest. This ensures that no additional noise from surrounding signals will be incorporated into the velocity-amplitude spectrum.

Thresholding and Profile Analysis

To differentiate the main velocity profile from lower-intensity, high-velocity regions (commonly referred to as LAHV—low amplitude high velocity), the user selects a velocity cutoff point by clicking on the image. This threshold is confirmed via a prompt and displayed on the image in red. The program then extracts pixel intensity data beyond the main dense spectral envelope and generates two graphs: the velocity profile vs. pixel intensity and maximum intensity for each velocity. This is accomplished via a nested for-loop that cycles through each row and column in the image and adds the velocity and intensity pairs into two empty arrays. These for loops include the conversion of each pixel value to a velocity value. In generating the first graph, these pairs are then plotted to create a scatter plot of all velocity-intensity pairs in the main profile. For the second graph, the maximum intensity that corresponds to each velocity value is added to a separate array, and these are plotted in order to calculate the AUC of the profile, quantifying the total intensity contribution of the flow profile.

Plateau Region and Thresholded AUC

For further analysis, the user selects the start and end points of a plateau region in the intensity-velocity plot, from which the average intensity is computed. The user then manually enters the velocity threshold value (as previously selected) to generate a thresholded AUC plot that excludes all velocities below the defined cutoff.

Data Export

Final output metrics, including AUC values and average intensities, are automatically exported to an Excel spreadsheet. Each analysis trial was saved as a new column, facilitating comparison across multiple regions or image trials.

Accessing the Materials

All MATLAB code developed for this project is available on GitHub at <https://github.com/lilythomson13/capstone>. The repository includes the main analysis script (Script.m), example Doppler image files, and instructions for setup and execution. Users are advised to download (not copy-paste) the .m file to ensure proper formatting and functionality. All input Doppler images used in this analysis are stored

locally due to privacy constraints but can be replaced with publicly available equivalents for demonstration purposes.

Users must ensure that the image files are placed in the same folder as the MATLAB script before execution. A detailed README file is included in the repository to guide users through the setup, image preprocessing, velocity calibration, and export steps.

Results

The Lindner lab performed comprehensive echocardiography on 30 patients enrolled in their clinical trial. We applied our program to these images, with the most important calculations being the LAHV AUC and LAHV AUC normalized to intensity.

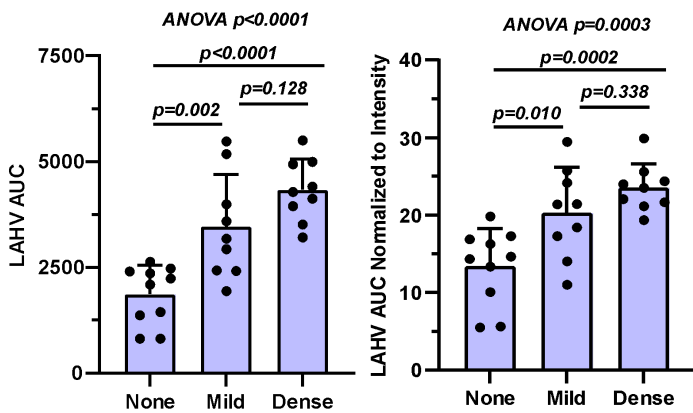


Figure 3. Kruskal-Wallis test on the LAHV AUC and the visual grading (left) and the LAHV AUC normalized to intensity and the visual grading (right).

An expert visual grader categorized each of these patient images as having none, mild, or dense LAHV signal. In order to compare continuous data to a categorical variable, we did a Kruskal-Wallis test on the LAHV AUC and the visual grading, as well as the LAHV AUC normalized to intensity and the visual grading (Figure 3). The results showed that patients visually identified as having LAHV domains had significantly higher AUC values than those without (3393 ± 1079 vs 1864 ± 693 , $p < 0.001$). Subjective LAHV grade correlated well with AUC ($p = 0.0002$) and AUC normalized to gain (average intensity of profile) ($p = 0.001$). While there is a significant difference between LAHV visually graded as none and mild and none and dense, there was not a significant difference between LAHV visually graded as mild and dense, in both the LAHV AUC and LAHV AUC normalized to intensity calculation.

Several shear-activation markers correlated linearly with LAHV AUC calculations (Supplementary

Figure 2). The markers with the greatest correlation are Pac-1 and RANTES (Figures 4 & 5).

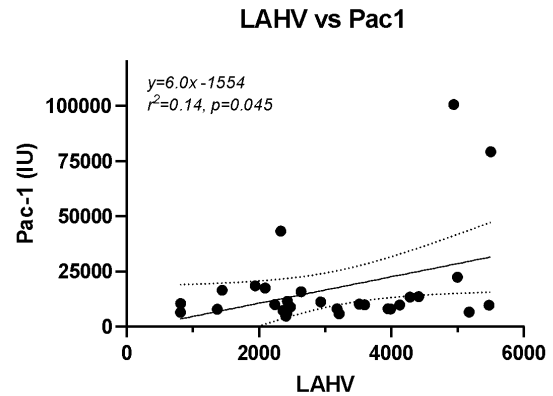


Figure 4. Scatter plot showing the relationship between LAHV AUC values and platelet activation marker Pac-1 (IU). A significant positive correlation was observed ($r^2 = 0.14$, $p = 0.045$), indicating that higher LAHV values are associated with increased platelet activation, consistent with heightened shear stress across the aortic valve.

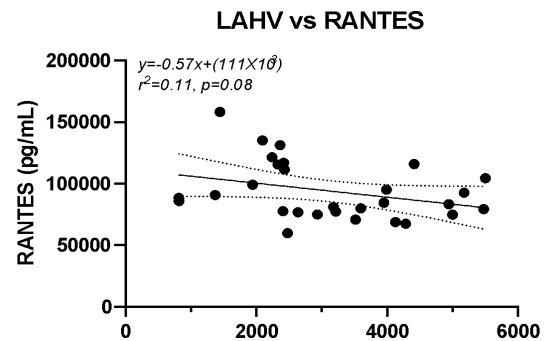


Figure 5. Scatter plot showing the relationship between LAHV AUC values and plasma RANTES (pg/mL). A modest negative correlation was observed ($r^2 = 0.11$, $p = 0.08$), suggesting that increased shear flow domains may be associated with reduced circulating RANTES.

Pac-1 is a receptor on platelets that is responsible for binding to extracellular matrix proteins like fibrinogen, which is essential for clot formation.¹⁸ The increased platelet activation caused by PAC-1 could contribute to the formation of thrombi (blood clots) in the aortic valve, further narrowing it and potentially leading to complications like heart failure. The increased LAHV AUC correlated with increased Pac-1 levels, with an R^2 of 0.14. RANTES, or CCL5, is a chemokine involved in inflammation and immune cell recruitment.¹⁸ Our results showed a negative correlation between LAHV AUC and

RANTES levels, with an R^2 of -0.11. This could possibly be because RANTES may be sequestered on endothelial surfaces or platelets at the site of disturbed flow, reducing its circulating plasma levels despite ongoing local activity in inflammation and platelet aggregation.

The LAHV values extracted from the program were quantitatively validated against profiles produced from a 4D Flow MRI of 3D-printed replicas from three patients. These studies use a pulsatile flow phantom, with the data shared by Dr. Jeesoo Lee from the Feinberg School of Medicine at Northwestern University. These early results from the 4D flow MRI show that peak shear appears to correlate with the larger LAHV AUC (Figure 6), further supporting the investigation of the LAHV regions corresponding with increased shear markers.

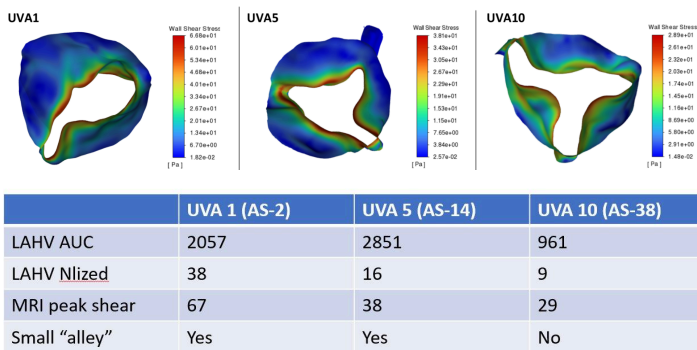


Figure 6. Preliminary 4D flow MRI results from three patients, showing their LAHV AUC, LAHV normalized to intensity, MRI peak shear, and the presence of small "alley's" in their valves.

Discussion

The MATLAB program developed for this capstone project effectively distinguished and quantified LAHV signals in Doppler echocardiograms of patients with AS. Furthermore, the statistically significant difference in the quantified AUC values between profiles with none and mild, and none and dense LAHV signal demonstrates this method can objectively separate groups that may otherwise be assessed subjectively (e.g., visually). It also demonstrates that this tool is sensitive enough to detect quantitative differences in LAHV patterns across different severities and proves that presence and intensity of LAHV signal is measurable, not just qualitative. Therefore, this supports the potential use of the tool as a quantitative aid in evaluating aortic stenosis severity, or at least as a supplementary metric for characterizing abnormal flow dynamics.

The results also correlated modestly with blood markers of increased valve shear stress. Specifically,

patients with larger LAHV AUCs demonstrated elevated levels of shear-sensitive blood markers, suggesting that the program captures physiologically meaningful flow characteristics. Thus, the LAHV AUC may serve as a quantitative proxy for shear-related blood changes, linking image data to real biochemical stress in patients. It is highly likely that most of the action with respect to the platelet activation, VWF adhesion, TGF signaling, and so on are going to be localized at the valve surface. Accordingly, we are limited in using the circulating markers to reveal these processes, which may make this approach useful since it provides information beyond what would be possible with a simple blood test. Thus, this prospective study looks into whether the LAHV or blood markers are the better predictor of AS progression in patients with mild or moderate AS. This also strengthens the validity of the tool, as it aligns image-based quantification with molecular evidence, and opens the door for this metric to be used in non-invasive monitoring of shear stress or even disease progression in AS patients. Moving forward, a full completion of the 4D flow analysis on all patients will be done to finalize the full correlation of this project's results.

Overall, this project addresses a gap in current ultrasound machines which can currently only measure a Doppler profile's mean and peak velocities. Additionally, these results contribute to a larger study being done by the Lindner Lab on AS and hopefully supports progress towards non-surgical, therapeutic interventions.⁴ The information on valvular microdomains of shear that produce LAHV signals could also promote the concept of "precision medicine" in AS by allowing clinicians to use specific therapies that target adverse shear-mediated signaling in AS. It could also be used in other applications, like the assessment of prosthetic heart valve function.

Future directions of this program include further development of its user interface design, possibly integrating it with existing ultrasound softwares, and further validation across a larger clinical trial framework. Right now, this MATLAB program relies on user interaction for ROI and threshold selection. For clinical deployment, this would need to be simplified into a graphical user interface with automated or semi-automated ROI detection to reduce inter-user variability and improve speed. The algorithm could be integrated into current ultrasound platforms through vendor-supported plug-ins, post-processing modules, or cloud-based analysis tools that interface with exported DICOM images. This would allow the tool to be more user-friendly and accessible to clinicians without technical training. Ultimately, embedding the algorithm into commercial ultrasound

platforms could enable real-time or near-real-time analysis at the bedside.

End Matter

Author Contributions and Notes.

The authors declare no conflict of interest.

Acknowledgments

Dr. Jonathan Lindner, MD, Cardiovascular Medicine

Dr. John Hossack, PhD, Emeritus Professor of Biomedical Engineering

Capstone Teaching Team (Dr. Allen, Mario Garcia, Hayley Sussman)

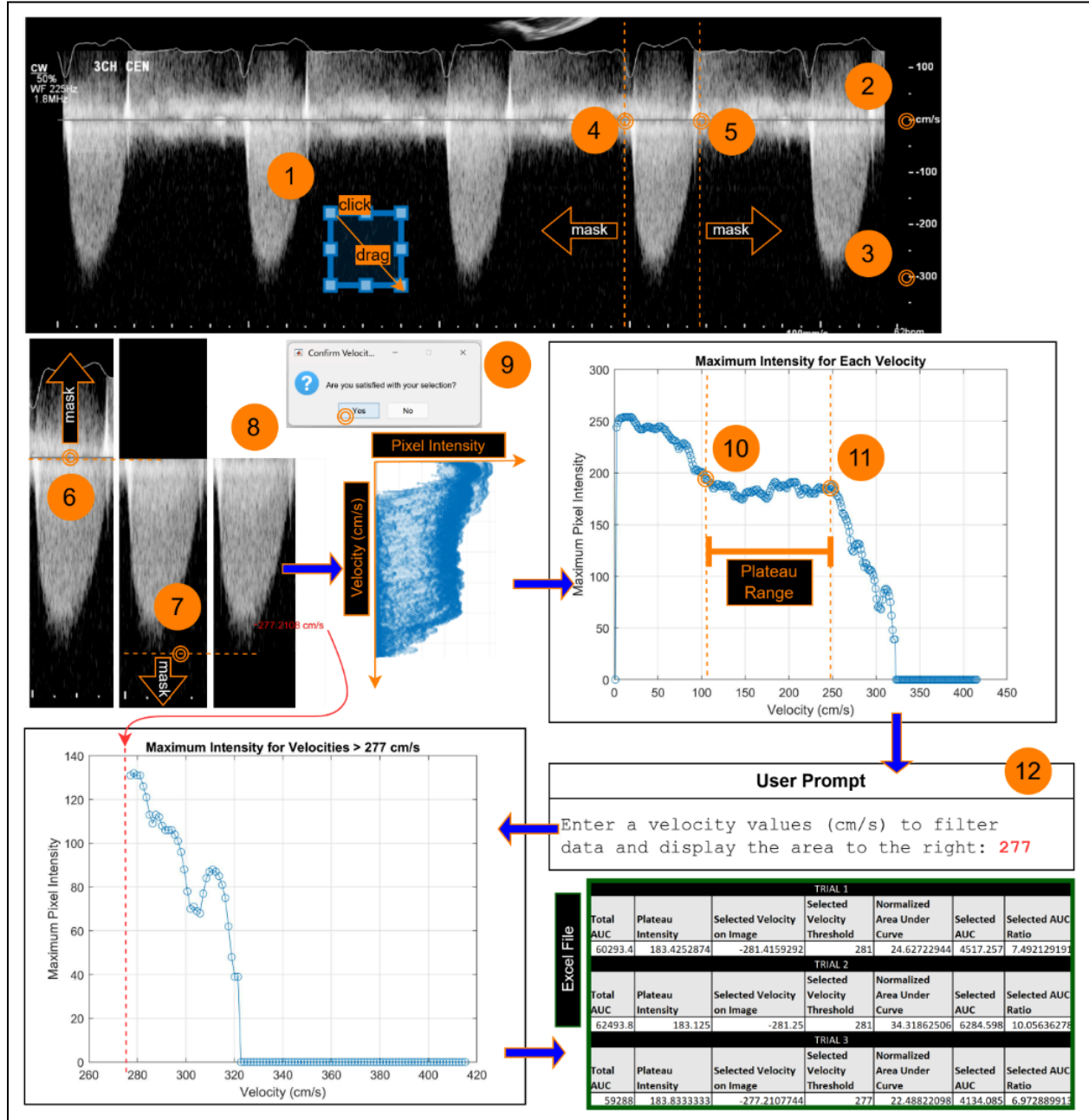
Funded by NIH Grant RO1-HL165422

References

1. Ancona R, Pinto SC. Epidemiology of aortic valve stenosis (AS) and of aortic valve incompetence (AI): is the prevalence of AS/AI similar in different parts of the world? *European Society of Cardiology*. Published February 12, 2020. <https://www.escardio.org/Journals/E-Journal-of-Cardiology-Practice/Volume-18/epidemiology-of-aortic-valve-stenosis-as-and-of-aortic-valve-incompetence-ai>
2. Mayo Clinic. Aortic valve stenosis - symptoms and causes. Published August 18, 2024. Accessed November 12, 2024. <https://www.mayoclinic.org/diseases-conditions/aortic-stenosis/symptoms-causes/syc-20353139>
3. Goody PR, Hosen MR, Christmann D, Niepmann ST. Aortic valve stenosis: from basic mechanisms to novel therapeutic targets. *Arteriosclerosis, Thrombosis, and Vascular Biology*. 2020;40(4). doi:10.1161/ATVBAHA.119.313067
4. Lindner JR. Advanced non-invasive imaging in the investigation of aortic stenosis pathobiology. *NIH RePORTER*. <https://reporter.nih.gov/search/7s-5CxuqB06PocT5RDYRew/project-details/10892832#description>
5. Mayo Clinic. Aortic valve stenosis - symptoms and causes. Published August 18, 2024. Accessed November 12, 2024. <https://www.mayoclinic.org/diseases-conditions/aortic-stenosis/symptoms-causes/syc-20353139>
6. Penn Medicine. Aortic valve stenosis. Published 2022. Accessed May 3, 2025. <https://www.pennmedicine.org/for-patients-and-visitors/patient-information/conditions-treated-a-to-z/aortic-valve-stenosis>
7. Pujari SH, Agasthi P. Aortic stenosis. *PubMed*. Published April 16, 2023. <https://www.ncbi.nlm.nih.gov/books/NBK557628/>
8. Penn medicine. Balloon valvuloplasty (valvotomy). Published 2023. Accessed May 3, 2025. <https://www.pennmedicine.org/for-patients-and-visitors/find-a-program-or-service/heart-and-vascular/heart-valve-disease/treatments-and-procedures/valvuloplasty>
9. American Heart Association. What is TAVR? Published 2018. Accessed November 12, 2024. <https://www.heart.org/en/health-topics/heart-valve-problems-and-disease/understanding-your-heart-valve-treatment-options/what-is-tavr>
10. Mayo Clinic. Aortic valve repair and aortic valve replacement. Published June 11, 2024. Accessed November 12, 2024. <https://www.mayoclinic.org/tests-procedures/aortic-valve-repair-aortic-valve-replacement/about/pac-20385093>
11. Mayo Clinic. Transcatheter aortic valve replacement (TAVR). Published September 6, 2023. Accessed November 12, 2024. <https://www.mayoclinic.org/tests-procedures/transcatheter-aortic-valve-replacement/about/pac-20384698>
12. Walter M. TAVR costs vary significantly from one hospital to the next. *Cardiovascular Business*. Published April 3, 2023. Accessed May 8, 2025. <https://cardiovascularbusiness.com/topics/clinical/structural-heart-disease/tavr/tavr-costs-vary-significantly-one-hospital-next>
13. Shah SM, Shah J, Lakey SM, Garg P, Ripley DP. Pathophysiology, emerging techniques for the assessment and novel treatment of aortic stenosis. *Open Heart*. 2023;10(1):e002244. doi:10.1136/openhrt-2022-002244
14. Marquis-Gravel G, Redfors B, Leon MB, Généreux P. Medical treatment of aortic stenosis. *Circulation*. 2016;134(22):1766-1784. doi:10.1161/circulationaha.116.023997
15. Ozawa K, Packwood W, Varlamov O, et al. Molecular imaging of VWF (von willebrand factor) and platelet adhesion in postischemic impaired microvascular reflow. *Circ Cardiovasc*

- Imaging*. 2018;11(11). Published November 15th, 2018. doi:10.1161/CIRCIMAGING.118.007913
16. Toronto General Department of Anesthesia. Virtual transesophageal echocardiography. Accessed November 12, 2024. https://pie.med.utoronto.ca/TEE/TEE_content/TEE_spectral_intro.html
 17. Cortes GA, Moore MJ, El-Nakeep S. Physiology von willebrand factor. In: *StatPearls*. StatPearls Publishing; 2025. Accessed May 7, 2025. <http://www.ncbi.nlm.nih.gov/books/NBK559062/>
 18. Taub R, Gould RJ, Garsky VM, et al. A monoclonal antibody against the platelet fibrinogen receptor contains a sequence that mimics a receptor recognition domain in fibrinogen. *J Biol Chem*. 1989;264(1):259-265.
 19. Stuart MJ, Baune BT. Chemokines and chemokine receptors in mood disorders, schizophrenia, and cognitive impairment: a systematic review of biomarker studies. *Neurosci & Biobehav Rev*. 2014;42:93-115. doi:10.1016/j.neubiorev.2014.02.001

Supplementary Material



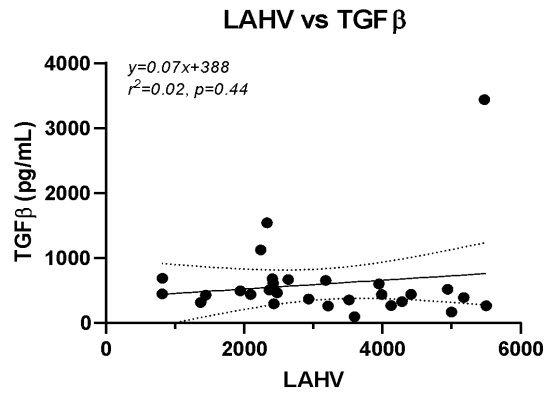
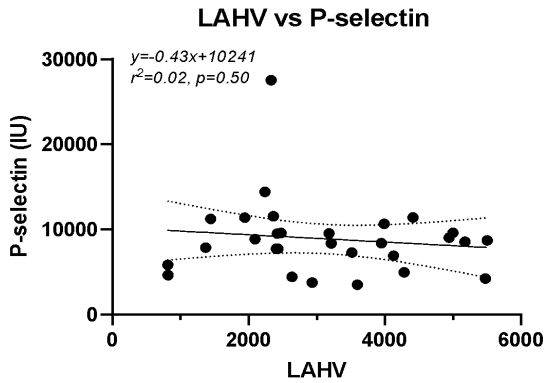
Supplementary Figure 1. Schematic of MATLAB Program Steps

Image pre-processing steps. (1) Highlight a rectangular area of the background space to average the intensities of, subtracting that average from the entire image. (2) Select “0 cm/s” on the image’s velocity scale. (3) Select “300” on the image’s velocity scale. (4) Select the left side of the profile of interest to mask everything to the left of it. (5) Select the right side of the profile of interest to mask everything to the right of it. (6) Select the baseline of the velocity profile to mask everything above it. (7) Select the lowermost horizontal axis of the image, closest to the profile end, to mask everything below it.

Analysis steps. (8) Click a point on the profile that aligns with your desired velocity cut-off value between the main profile and low amplitude (or intensity), high velocity (LAHV) region. The selected velocity value will display on image in the color red. (9) Confirm the choice by clicking “Yes” in the pop-up box

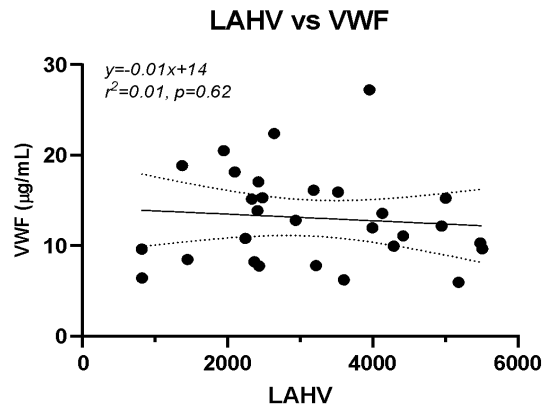
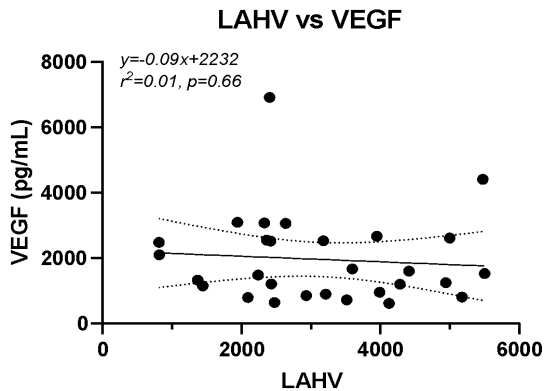
to proceed or clicking “No” to redo the selection. Then, the program generates a graph of the signal's velocity profiles versus the pixel intensity. A graph of the maximum pixel intensity for each velocity value is then presented. (10) Click to the left (11) then right of this graph's plateau region to calculate the average intensity value of this range. (12) Type the velocity threshold value that aligns with the one displayed in red on the profile's image in step 8. A graph of the maximum intensities greater than the inputted velocity displays, and its AUC is calculated. This value and others are automatically exported to an Excel file.

Supplementary Figure 2. Shear-Activation Markers vs LAHV AUC



Supplementary Fig 2a. LAHV vs P-selectin (IU)

Supplementary Fig 2b. LAHV vs TGF β (pg/mL)



Supplementary Fig 2c. LAHV vs VEGF (pg/mL)

Supplementary Fig 2d. LAHV vs VWF (μ g/mL)